Journal of Medicinal Chemistry

pubs.acs.org/jmc

Article

Rhodium(III) Complex Noncanonically Potentiates Antitumor Immune Responses by Inhibiting Wnt/β-Catenin Signaling

Feng-Yang Wang,[§] Liang-Mei Yang,[§] Xiao-Lin Xiong,[§] Jing Yang, Yan Yang, Jiu-Qin Tang, Lei Gao, Yuan Lu, Yuan Wang, Taotao Zou,* Hong Liang,* and Ke-Bin Huang*

Cite This: J. Med. Chem. 2024, 67, 13778−13787

Read Online

ACCESS | Metrics & More | Article Recommendations | Supporting Information

ABSTRACT: Metal-based chemoimmunotherapy has recently garnered significant attention for its capacity to stimulate tumor-specific immunity beyond direct cytotoxic effects. Such effects are usually caused by ICD via the activation of DAMP signals. However, metal complexes that can elicit antitumor immune responses other than ICD have not yet been described. Herein, we report that a rhodium complex (**Rh-1**) triggers potent antitumor immune responses by downregulating Wnt/β-catenin signaling with subsequent activation of T lymphocyte infiltration to the tumor site. The results of mechanistic experiments suggest that ROS accumulation following **Rh-1** treatment is a critical trigger of a decrease in β-catenin and enhanced secretion of CCL4, a key mediator of T cell infiltration. Through these properties, **Rh-1** exerts a synergistic effect in combination with PD-1 inhibitors against tumor growth *in vivo*. Taken together, our work describes a promising metal-based antitumor agent with a noncanonical mode of action to sensitize tumor tissues to ICB therapy.

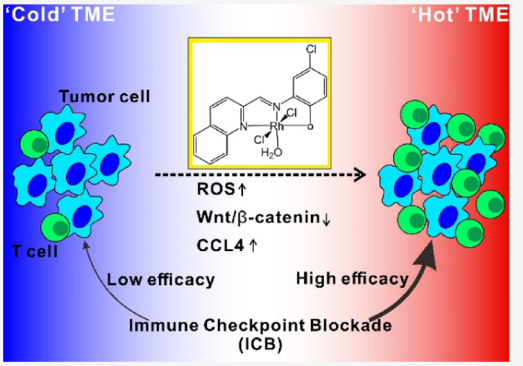

1. INTRODUCTION

Several specific, metal-based agents have been reported to exhibit cytotoxicity, provoking anticancer immunity.[1−4] A typical mechanism of these complexes is known as immunogenic cell death (ICD), in which the drug-treated tumor tissue promotes T cell proliferation, which is dependent on the antigen-presenting process from dendritic cells (DCs) activated by the immunostimulatory signal, including cell surface exposure of calreticulin (CRT), secretion of high mobility group box 1 (HMGB1), and release of ATP.[5−9] In recent years, an increasing number of metal complexes, based on platinum, iridium, gold, ruthenium, and copper, that exhibit potent ICD activity, have been developed.[10−26] Importantly, synergistic antitumor effects have also been confirmed when combining metal-based ICD agents with immune checkpoint blockade (ICB) therapeutics, as exemplified by the use of oxaliplatin with PD-1 inhibitors.[27,28] Beyond their role in ICD, metal complexes have demonstrated the ability to modulate inflammation or immune responses through diverse pathways, including regulating zinc homeostasis, targeting specific proteins, etc.[29−33]

In addition to the activation of T cells through the antigen-presenting process, the success of tumor cell eradication is also dependent on a sufficient number of tumor-infiltrating lymphocytes (TILs).[34−36] However, a variety of evasion strategies by which tumor cells reduce T cell infiltration have been described.[37−39] Of these, the Wnt/β-catenin pathway has been identified as one of the most crucial oncogenic signaling pathways associated with immune evasion.[40−43] For example, β-catenin inhibits the transcription of CCL4-mediated infiltration and activation of $CD103^+$ DCs and $CD8^+$ T cells, leading to a subsequent lack of response to immune checkpoint blockade.[44] A couple of studies have confirmed the ability of metal compounds to inhibit the Wnt/β-catenin pathway;[45,46] however, whether the antitumor immunity could be achieved by these metal-based agents remained unknown. In view of their high structural diversity and tight relationship with antitumor immunity as reported, metal complexes would offer a suitable pool for mining new Wnt/β-catenin pathway inhibitors with potent immunostimulatory activity.

Rhodium complexes have shown promising anticancer activity, but few studies have reported their biological mode(s) of action.[47−51] Here, we screened a series of rhodium compounds and identified a potent Wnt/β-catenin pathway inhibitor, **Rh-1**. We found that ROS accumulation was a key event in β-catenin blockage and CCL4 secretion. Moreover, **Rh-1** potentiated the PD-1 blockade in inhibiting tumor growth in animal models. Similarly, we observed the manifestation of this synergistic effect as enhanced T cell

Received: March 10, 2024
Revised: July 2, 2024
Accepted: August 1, 2024
Published: August 12, 2024

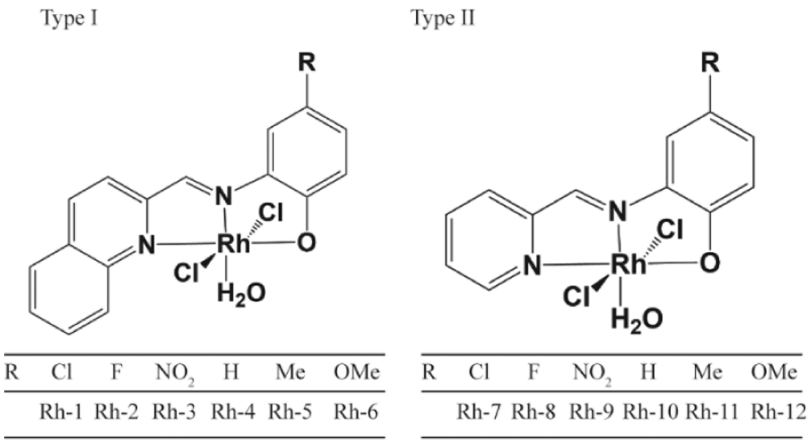

Figure 1. Chemical structures of the Rh(III) complexes.

infiltration by **Rh-1**-stimulated CCL4 secretion in the tumor microenvironment. Based on our findings, **Rh-1** or similar metal-based Wnt/β-catenin inhibitors may emerge as chemotherapeutic agents to complement current or future ICB therapeutic strategies.

2. RESULTS AND DISCUSSION

2.1. Synthesis and Characterization. Reedijk and coworkers have reported that 4-methyl-2-N-(2-pyridylmethyl)-aminophenol (Hpyrimol) coordinated with copper, iron, zinc, et al. could result in multiple biological synergistic effects.[52−54] Based on the theory of structure−activity relationship, we synthesized 12 new ligands based on the Hpyrimol structure, and then 12 novel rhodium(III) complexes have also been synthesized (Figure 1) and fully characterized by ^{1}H NMR, ^{13}C NMR and ESI-MS (see details in the synthetic section, Supporting Information). We also performed X-ray crystallography on **Rh-1** and **Rh-5**. According to the X-ray crystallography data (Table S1), the Rh(III) metal center is coordinated by two Cl^{-} ions, one H_2O molecule, and two N atoms and one O atom from the tridentate ligand. Two five-membered chelating rings are formed and share the common Rh−N edge in the two complexes (Figures 2 and S51). The rhodium(III) metal center shows a twisted octahedral configuration with the six coordination mode, in which the metal center and tridentate ligand form a planar structure. These metal complexes are mainly divided into two categories based on the different core nitrogen heterocycles including quinoline and pyridine, and they differ in the substituent groups of the benzene rings, which can affect the lipophilicity and electronic effects in a series of structures with the same N heterocycle. These substitution groups are also mainly divided into two categories: electron-withdrawing groups containing Cl, F and NO_2, and electron-supplying groups containing H, Me and OMe. These rhodium(III) complexes dissolved readily in common organic solvents, such as DMF and DMSO, and are soluble in PBS after dilution from DMF stock solution (1% DMF unless otherwise stated).

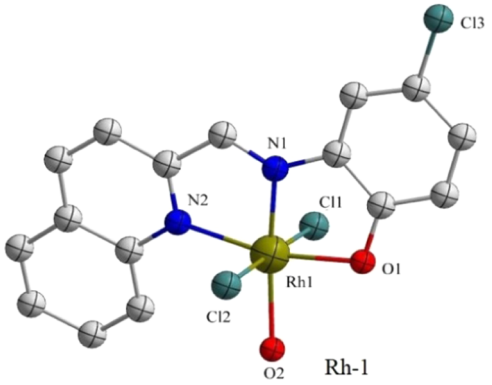

Figure 2. X-ray crystallography structure of **Rh-1** at a 50% probability level. All hydrogen atoms were removed for clarity.

2.2. Stability of Rh Complexes. The stability of Rh complexes was investigated using HPLC and UV absorption spectroscopy under physiological conditions (Tris-KCl-HCl buffer, pH 7.35). As illustrated in Figures S52 and S53 (Supporting Information), the time-dependent HPLC chromatograms (12, 24, and 48 h) demonstrate that there are no observable changes in the incubation solution. This indicates that the Rh complexes remained stable in the TBS buffer for up to 48 h at room temperature. To further validate the HPLC results, the time-dependent UV absorption spectra of the Rh complex were also monitored, as shown in Figure S54. The UV absorption spectra showed no significant red or blue shifts after incubation for different durations under physiological conditions. This further corroborates the reliability of the HPLC test results.

2.3. *In Vitro* Cytotoxic Activity of Rhodium(III) Complexes. We investigated the *in vitro* cytotoxicity of the rhodium complexes and their ligands in triple-negative breast cancer (TNBC, 4T1 and MDA-MB-231), urinary bladder cancer (T-24), liver cancer (BEL-7404 and HepG2) and gastric cancer (MGC-803) cell lines. None of the ligands or $Rh(III)Cl_3$ salt elicited cytotoxicity against the tested cell lines (IC_{50} > 40 μM), but almost all rhodium complexes showed some degree of cytotoxicity against all tested cancer cell lines (IC_{50} values ranging from 2.48 to 25.61 μM), indicating that the coordination between the ligands and metal salt exhibited a cytotoxic synergism. As shown in Table S2, the IC_{50} values of the rhodium complexes with electron-withdrawing groups were significantly lower than those of the rhodium complexes with electron-donating groups in all tested cell lines, among which two complexes with chlorine atoms are the most toxic against TNBC cell lines (IC_{50} values of 2.48−4.56 μM for Rh-1 and 6.34−6.78 μM for Rh-7). In addition, quinine-based rhodium complexes (Rh-1-6) tended to exhibit higher activities against a given cell line than the pyridine-based rhodium complexes

https://doi.org/10.1021/acs.jmedchem.4c00583
J. Med. Chem. 2024, 67, 13778−13787

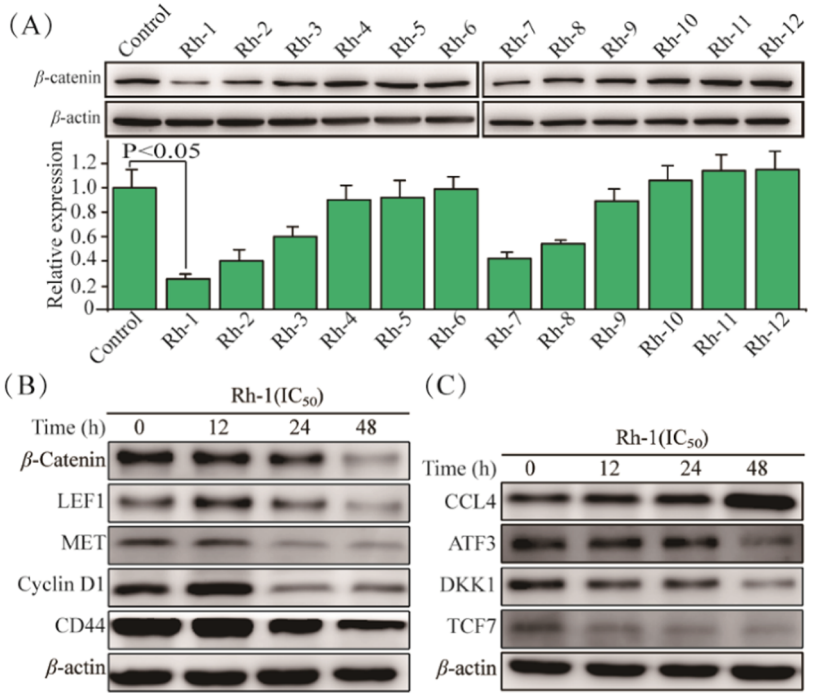

Figure 3. (A) Western blot analysis of β-catenin protein after treatment with 12 different Rh(III) complexes; (B−C) Western blot analysis of proteins related to Wnt/β-catenin signaling and chemokine CCL4 after treatment with **Rh-1**.

(Rh-7-12) with the same R group. The difference in cytotoxicity among rhodium complexes may be attributed to the varying lipophilicity or electronic effects of their ligands. **Rh-1** showed the strongest activity (IC_{50} value of 2.48 μM) out of all the complexes against TNBC 4T1 cell line, which was also more potent than that of the positive control, cisplatin (IC_{50} value of 4.21 μM). In addition, the IC_{50} values of **Rh-1** against different cancer cell lines exhibited apparent differences (IC_{50} values ranging from 2.48 to 13.02 μM), suggesting a certain extent of selectivity to cancer cell types. Considering the excellent cytotoxicity of **Rh-1** against 4T1 cell line and the fact that TNBC is a type of highly aggressive cancer that is hard to be cured, 4T1 cell line was chosen for further study.

2.4. Inhibition of Wnt/β-Catenin Signaling: Candidate Screening. In addition to cytotoxicity, we also sought to identify a candidate inhibitor of Wnt/β-catenin signaling to potentially stimulate anticancer immunity against TNBC. To this end, we treated 4T1 cells with the 12 compounds (at their IC_{50} concentrations) for 48 h, and then examined β-catenin expression, a key component of the Wnt signaling pathway, by Western blot analysis. As shown in Figure 3A, rhodium complexes with an electron-withdrawing group (R) showed differing downregulation of the β-catenin protein. In particular, two rhodium complexes with chlorine groups, **Rh-1** and **Rh-7**, exhibited the most significant inhibition of Wnt/β-catenin signaling. Due to the apparent downregulation of β-catenin and excellent cytotoxicity induced by **Rh-1** against the 4T1 cell line, we chose this complex as a representative rhodium compound for subsequent experiments aimed at elucidating the mechanism(s) of cytotoxicity and immune-regulation in the 4T1 cancer cell line.

Further confirming the downregulation of Wnt/β-catenin signaling induced by **Rh-1**, we observed a time-dependent downregulation of the protein levels of two target genes in the Wnt/β-catenin pathway, the receptor tyrosine kinase (MET) and lymphoid enhancer-binding factor 1 (LEF1), after treatment with **Rh-1**. We also observed downregulation of the transcription of two Wnt-dependent genes, dickkopf 1 (DKK1) and cyclin D1, and the protein levels of the related transcription factor, T cell factor 7 (TCF7), and CD44 upon treatment with **Rh-1** (Figure 3B,C).[40−43] These data indicate that the Wnt/β-catenin signaling pathway is substantially inhibited by **Rh-1**.

Previous studies have shown that Wnt signaling downregulation can improve T cell recruitment or infiltration, since downregulated Wnt/β-catenin signaling inhibits the expression of the transcriptional repressor, activating transcription factor 3 (ATF3), and that ATF3 inhibition can promote CCL4 production, which is a chemokine-associated with T-cell infiltration or recruitment in tumors.[44] Therefore, we next pursued whether Wnt/β-catenin signaling regulated by **Rh-1** promotes CCL4 production. Consistent with the previous study, we observed decreased ATF3 and increased CCL4 expression in tumor cells treated with **Rh-1** (Figure 3C), indicating that **Rh-1** has the potential to promote T cell infiltration of tumors.

2.5. Mechanism of Rh-1 Regulating Wnt/β-Catenin Signaling. Some metal complexes with anticancer activity stimulate ROS production and induce ER-stress.[55−58] Previous studies have also indicated that ER stress can result in downregulation of Wnt/β-catenin signaling, since activating transcription factor 4 (ATF4), an ER stress-inducible transcription factor, can promote the expression of C/EBP homologous protein (CHOP).[59,60] CHOP acts as a specific inhibitor of Wnt-TCF signaling, since this inhibition blocks the binding of TCF to its DNA recognition site.[61,62] Therefore, we examined whether the downregulation of β-catenin protein induced by **Rh-1** is related to ER-stress. After incubation of 4T1 cells with 3 μM **Rh-1** for 0−48 h, the expression levels of phosphorylated RNA-dependent protein kinase-like endoplasmic reticulum kinase (PERK), phosphorylated eukaryotic initiation factor 2a (eIF2a), and CHOP all showed time-

https://doi.org/10.1021/acs.jmedchem.4c00583
J. Med. Chem. 2024, 67, 13778−13787

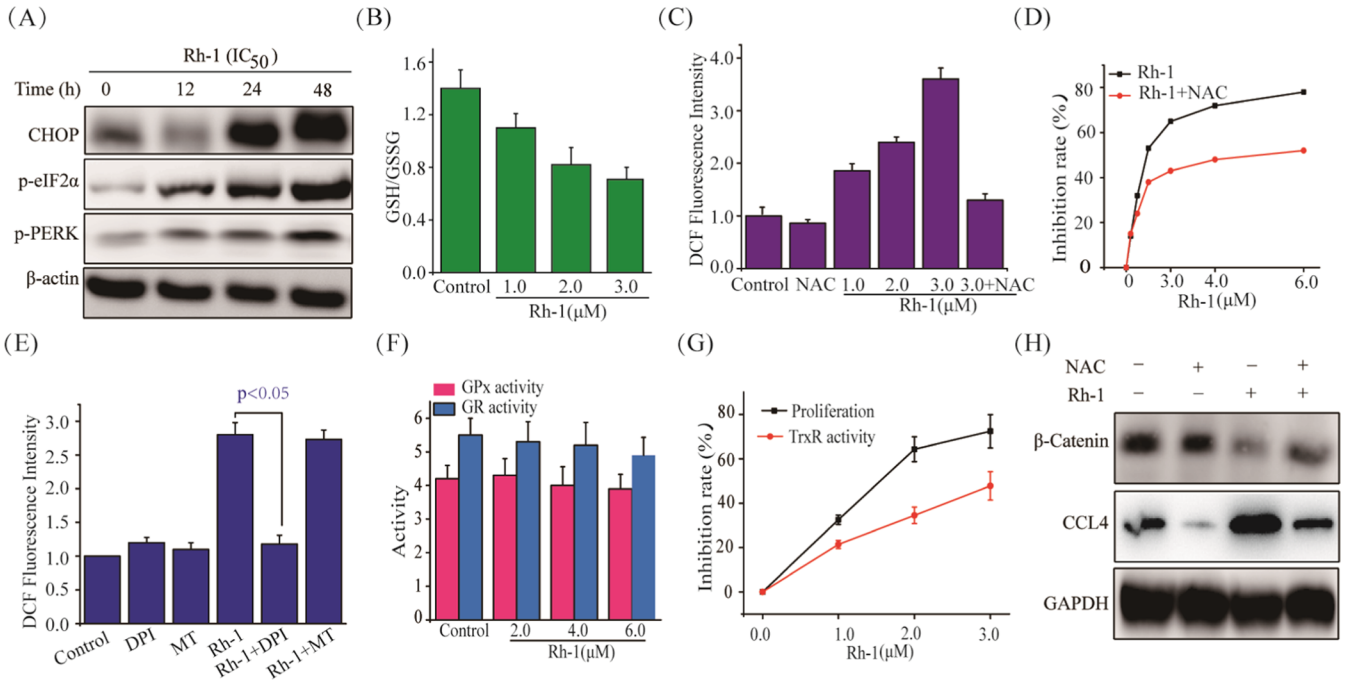

Figure 4. (A) WB analysis of ER-stress-related proteins in 4T1 cells treated with **Rh-1** (at the IC_{50} concentration) for the indicated durations; (B) The ratio of reduced glutathione (GSH) to oxidized glutathione (GSSG) significantly decreased after **Rh-1** treatment; (C) Representative histogram plot of ROS stained by DCF-DA. Pretreatment with the antioxidant (NAC, 5 mM) resulted in a reduction of the ROS levels induced by **Rh-1**; (D) Proliferative inhibition by **Rh-1** was significantly lower in the presence of 5 mM NAC compared with **Rh-1** alone; (E) The ROS induced by 3 μM **Rh-1** was inhibited by the NADPH oxidase inhibitor, DPI and MT. The data are shown as mean ± std, $n \geq 3$, DPI, diphenylene iodonium chloride; MT, mito-tempo; (F) GSH peroxidase and reductase activities were examined in the presence of **Rh-1**; (G) TrxR activity inhibition occurred approximately in parallel with the proliferative inhibition of 4T1 cells upon **Rh-1** treatment; (H) Western blot analysis of proteins related to ROS and the downregulation of β-catenin and CCL4.

dependent increase (Figure 4A), indicating the induction of ER-stress. The ER-stress response plays a critical role in triggering various cell death pathways. Particularly, apoptosis is considered to be one of the significant death pathways resulting from the ER-stress response.[55−58] Thus, we examined the activation of caspase family proteins associated with apoptosis. We observed elevated caspase-3 and caspase-9 proteolytic activities following treatment with 3 μM **Rh-1** (Figure S55), indicating that **Rh-1** induces apoptosis which may be mediated by the ER-stress response. To understand the mechanism of **Rh-1**-induced ER-stress, we assessed ROS production. The ratio of intracellular GSH to GSSG, which is inversely related to ROS production,[63,64] was significantly decreased after treatment with **Rh-1** (Figure 4B). Consistent with this finding, the ROS scavenger, N-acetylcysteine (NAC), decreased ROS production and growth inhibition by **Rh-1** in 4T1 cells (Figure 4C,D). To further identify the source of ROS, we used two more ROS scavengers, DPI and MT, which are cognate inhibitors of NADPH oxidase and mitochondria, respectively.[65] Surprisingly, MT did not affect ROS level, while DPI significantly decreased the ROS (Figure 4E). Together, these results indicate that ROS production induced by **Rh-1** may be dependent on the SOD system, rather than mitochondrial damage. Antioxidant protein, glutathione peroxidase (GPx), can decrease ROS, oxidizing GSH to GSSG, which is then replenished by glutathione reductase (GR) that reduces GSSG back to GSH. Peroxiredoxin, one of the substrates of Trx, which can be reduced by TrxR, may also decrease ROS. Thus, the combined intracellular activities of TrxR, GPx, and GR make up the main antioxidant systems that impact ROS accumulation in cells.[66−71] After treating cells with **Rh-1** for 24 h, GPx activity was slightly decreased and GR activity remained nearly unchanged. In contrast, TrxR activity was dose-dependently inhibited after the 24 h treatment, along with inhibition of cell proliferation (Figure 4F,G), indicating that TrxR may be the target of **Rh-1**. In addition, the expression of TrxR was found to be significantly down-regulated by **Rh-1** treatment, in a time-dependent manner (Figure S56), indicating that **Rh-1** not only inhibited TrxR activity but also decreased TrxR expression, disrupting intracellular redox balance. Cisplatin and oxaliplatin are clinical metal-based drugs that can induce ROS production. However, oxaliplatin could not inhibit β-catenin expression (Figure S57), and the downregulation of β-catenin expression by cisplatin was much lower than that by Rh-1 (Figures 3B and S58). To further understand the role of TrxR inhibition in β-catenin suppression, we next compared β-catenin expression in 4T1 cells treated with auranofin and the gold(III) porphyrin [Au(TPP)]Cl. Auranofin, a classical metal-based inhibitor of TrxRs,[71] showed notable efficacy in suppressing β-catenin. In contrast, [Au(TPP)]Cl, another metal-based agent with weaker activity than that of auranofin against TrxRs,[71] failed to decrease β-catenin (Figure S58). Taken together, these data indicate that targeting TrxR may be a general trigger for β-catenin downregulation. Since ROS production is a common outcome of TrxR inhibition, we next sought to figure out the role of ROS in Wnt/β-catenin signaling. ER-stress-related proteins, apoptosis-related proteins, β-catenin, and chemokine CCL4 were inhibited after pretreating cells with NAC (Figures 4H, S55 and S59). Together, these results indicate that **Rh-1** may cause the inhibition of Wnt/β-catenin signaling, CCL4

https://doi.org/10.1021/acs.jmedchem.4c00583
J. Med. Chem. 2024, 67, 13778−13787

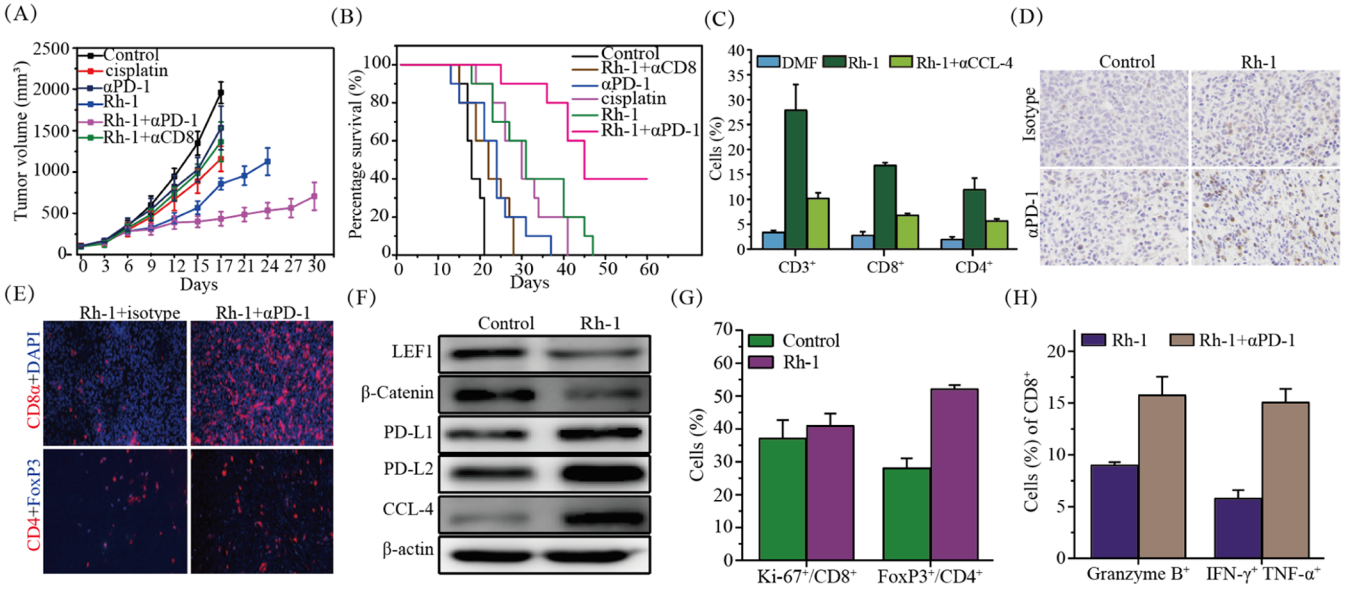

Figure 5. Induction of antitumor immune cell infiltration *in vivo*. (A) Tumor volumes of BALB/c mice bearing 4T1 cells (n = 7) after treatment with the indicated formulations; (B) Survival of BALB/c mice bearing 4T1 cells (n = 7) after treatment with the indicated formulations; (C) Flow cytometry analysis of T cell types in 4T1 tumors of BALB/c mice after treatment with **Rh-1**; (D) IHC analysis of $CD3^+$ T cells in tumors from mice treated with **Rh-1** or αPD-1 therapy alone or combined therapy; (E) IFC analysis of $CD8^+$ T cells and $CD4^+$ $FoxP3^+$ T cells in tumors from mice treated with **Rh-1** alone or combined therapy with **Rh-1** and αPD-1; (F) WB analysis of proteins involved in Wnt signaling, CCL4 and immune checkpoint PD-L1 and PD-1; (G) Flow cytometry analysis of K_i-67^+ in $CD8^+$ T cells and $CD4^+FoxP3^+$ T cells in 4T1 tumors from BALB/c mice after treatment with **Rh-1**; (H) Flow cytometry analysis of Granzyme B^+ and IFN-γ^+ TNF-α^+ in 4T1 tumors from BALB/c mice after treatment with **Rh-1** or combined **Rh-1** and αPD-1.

production, and ER-stress-dependent apoptosis as the ultimate consequences of ROS production.

2.6. *In Vivo* Chemoimmunotherapy Activity. To study the *in vivo* response of 4T1 tumors to **Rh-1**, we subcutaneously implanted mice with 8×10^4 4T1 cells and allowed the tumors to grow to approximately 60 mm^3 before treatment. The chemotherapy agent, cisplatin, which is effective in breast cancer patients, was used as a control. Cisplatin (2 mg/kg) or **Rh-1** (6 mg/kg) was administered (i.p.) once every 2 days. **Rh-1** treatment led to significantly slower tumor growth and increased survival compared with that of both control mice and cisplatin-treated mice (Figure 5A,B), meanwhile, no obvious organ toxicity was observed (Figure S60). β-catenin suppression is known to be associated with immune responses.[40−43] We assessed the effects of **Rh-1** on T cells in murine 4T1 tumors and found a significant increase in the number of $CD3^+$ T cells that were predominantly composed of $CD3^+$ $CD8^+$ cells (Figures 5C and S61) after 7 days of treatment. Next, we tested whether $CD8^+$ T cells were critical for the therapeutic benefits of **Rh-1**. To this end, we administered an anti-CD8 antibody to shield the function of $CD8^+$ T cells on days 3, 7, and 11 after the start of **Rh-1** treatment. The depletion of $CD8^+$ T cells abrogated the **Rh-1**-induced increase in survival and inhibition of tumor growth, with most mice dying within 20 days after tumor implantation, whereas most mice survived past 30 days with **Rh-1** treatment in the absence of the antibody (Figure 5B). Thus, $CD8^+$ T cells are critical for the efficacy of **Rh-1** therapy in this mouse model of breast cancer, while $CD4^+$ T cells are less important (Figures 5C and S61). When assessing the proliferation potential of $CD8^+$ TILs, we did not find obvious incensement in the expression of the nuclear proliferation marker, K_i-67, in $CD8^+$ TILs in mice administered **Rh-1** (Figures 5G and S62), but treatment with the formulation led to an increase in $CD4^+FoxP3^+$ Treg cells (Figures 5G and S62) as well as PD-L1 and PD-L2 expression in the tumor microenvironment (Figure 5F). Together, these data indicate that $CD8^+$ T cells infiltrate into breast tumors under **Rh-1** treatment, but the tumor microenvironment is still immunosuppressive. In addition, the key proteins of the Wnt signaling pathway, β-catenin, and LEF1, are significantly downregulated, while the CCL4 chemokine that promotes T-cell infiltration or recruitment in tumors is increased (Figure 5F), all of which is consistent with the results of the *in vitro* experiments (Figure 3C). For the role of CCL4 in T cell recruitment, we administered an anti-CCL4 antibody to shield its function on days 3, 7, and 11 after the start of **Rh-1** treatment. The T cells in tumors treated with **Rh-1** plus the anti-CCL4 antibody were lower than under treatment with **Rh-1** alone (Figure 5C). These data indicate that CCL4 is an important chemokine promoting T cell infiltration. We next examined the possibility that the antitumor immunity following **Rh-1** administration is from the classical immunogenic cell death (CICD) pathway by detecting HMGB-1, an important hallmark of CICD.[59,60] The secretion of HMGB-1 into the culture media by 4T1 cells treated with **Rh-1** (3.0 μM) for 24 or 48 h was not significantly altered, as determined by ELISA. Taken together, the above results suggest that **Rh-1** stimulates anticancer immunity primarily by affecting the Wnt signaling pathway.

Given the recent clinical success of PD-1 blockade and the PD-L1 promoting effect of **Rh-1**, we hypothesized that immune checkpoint blockade would synergize with **Rh-1** therapy to enhance antitumor immunity by boosting $CD8^+$ T-cell response. Treatment with anti-PD-1 alone did not obviously affect tumor growth or survival (Figure 5A,B). Notably, combining PD-1 pathway blockade (utilizing an anti-PD1 antibody) with **Rh-1** resulted in a substantial delay in tumor growth and enhanced survival compared to either

https://doi.org/10.1021/acs.jmedchem.4c00583
J. Med. Chem. 2024, 67, 13778−13787

therapy alone. Approximately 30% of the mice survived beyond 60 days and achieved complete remission (Figure S64), whereas none of the mice in the **Rh-1** group survived past 50 days (Figure 5A,B). We observed minimal to no increase in $CD3^+$ T cells in tumors treated with anti-PD-1 treatment alone, but combining **Rh-1** with anti-PD-1 led to a significant increase in $CD3^+$ T cells, compared with any of the monotherapy formulations (Figure 5D). Combination therapy also led to a substantial increase in $CD8^+$ T cells in the tumor compared with **Rh-1** alone (Figure 5E) with no difference in $CD4^+$ $FoxP3^+$ Treg cells in the tumor. We also found an increased fraction of granzyme B-producing $CD8^+$ T cells, as well as polyfunctional $CD8^+$ T cells producing both IFN-γ and TNF-α, in the mice treated with anti-PD-1 and **Rh-1** (Figures 5H and S63). Together, these results indicate that the intratumoral $CD8^+$ T-cell response is synergistically enhanced by combination therapy with **Rh-1** with anti-PD-1.

3. CONCLUSIONS

In summary, we identified a rhodium complex, **Rh-1**, as a new Wnt/β-catenin pathway inhibitor. This inhibition was achieved by cellular ROS production triggered by **Rh-1** (Scheme 1). As

Scheme 1. Graphic Summary of Rh-1-Induced Antitumor Immunity

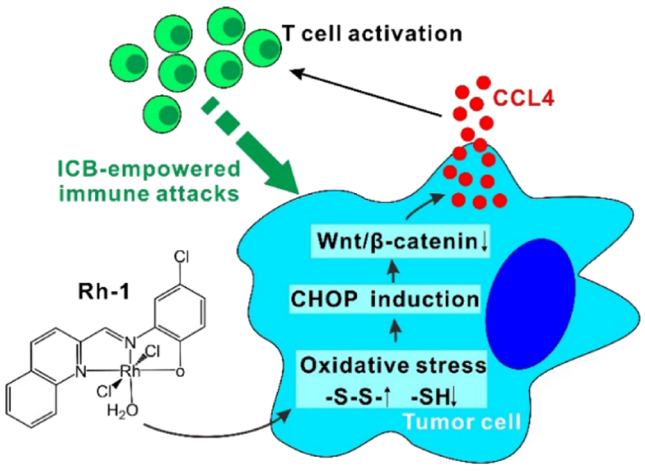

an outcome of Wnt/β-catenin inhibition, CCL4 is up-regulated to promote T cell infiltration into the tumor tissue, along with markers of activated $CD8^+$ T cells, such as granzyme B, IFN-γ, and TNF-α. Experiments using **Rh-1** with a PD-1 inhibitor demonstrated their synergism in combating tumor progression. Although the molecular basis behind this ROS-dependent inhibition of Wnt/β-catenin signaling warrants additional study, this work is instructive for the future design of metal-based agents with better performance.

Despite the significant success of combining ICD agents with cancer immunotherapy strategies, emerging mechanisms that reduce the ICD effect have been identified in certain cancer types.[72,73] Therefore, metal complexes with novel proinflammatory functions, such as **Rh-1**, will be important to overcoming the ongoing resistance to existing cancer chemo-immunotherapies.

4. EXPERIMENTAL SECTION

The relative purity of all target compounds used in the biophysical and biological studies was ≥95%, which were routinely confirmed by HPLC (waters e2695).

4.1. Materials and Reagents. The cancer cell lines including T-24, BEL-7404, MGC-803, HepG2, MDA-MB-231, 4T1 in this study were obtained from the Laboratory Cell Service Center at Chinese Academy of Sciences (Shang Hai, China). BALB/c mice at the age of 4 weeks were purchased from Changsha's animal research center (Hu Nan, China). Dulbecco's Modified Eagle Medium (DMEM), Roswell Park Memorial Institute 1640 Medium (RPMI 1640), and fetal bovine serum (FBS) were procured from Gibco Company. Penicillin, streptomycin, and trypsin were obtained from HyClone Company. Penicillin, streptomycin and trypsin were purchased from HyClone Company. Ethidium Homodimer-1 (EthD-1) and Calcein-AM were from Abbkine (USA) and Aladdin (Shanghai, China). Bovine albumin (BSA) and methylthiazolyldiphenyl-tetrazolium bromide (MTT) were obtained from Sigma. Human serum albumin (HSA) was purchased from Solarbio (Beijing, China). The following antibodies were used for Western Blot: p-eIF2α (#3398), p-PERK (#675505), CHOP (#5554), β-catenin (#862601), LEF1 (#653101), LEF1 (#653101), MET (#689902), Cyclin D1 (#681902), CD44 (#ab243894), β-actin (#664801), β-catenin (#862601), ATF3 (#ab254268), TCF7 (#615701), DKK1 (#PA5-23187), CCL4 (#710391), PD-L1 (#60475), PD-L2 (#49189). All chemicals, unless otherwise noted, were from commercial sources.

4.2. Synthesis and Characterization. General procedures for the synthesis of metal Rh complexes are illustrated below. Equimolar amounts (0.1 mol) of quinoline-2-carbaldehyde or pyridine-2-carbaldehyde and 2-amino-phenol derivatives in methanol were reacted for 4 h at 60 °C. After cooling, the solution was filtered and evaporated under reduced pressure. The crude product was recrystallized from CH_3OH/*n*-hexane. Next, the ligands (1 mmol) and $RhCl_3{\cdot}3H_2O$ (2 mmol) were dissolved in 15 mL $CH_3OH/CHCl_3$ solution (v/v = 3:2), and the mixture was stirred at 60 °C for 8 h. The resulting yellow solution was filtered and crystals or solid powders were obtained by slow evaporation of the solvent. For detailed data and spectra of all compounds, please refer to the corresponding part of Supporting Information.

4.3. Cytotoxicity Assay. The tested cancer cell lines included TNBC (4T1 and MDA-MB-231), urinary bladder cancer (T-24), liver cancer (BEL-7404 and HepG2) and gastric cancer (MGC-803) cell lines. Our previously published papers can be referred for the detailed cell culture conditions and screening methods cytotoxicity.[12]

4.4. *In Vivo* Mouse Studies. To test the acute toxicity of **Rh-1**, six-week-old male and female BALB/c mice, weighing 20−22 g, were randomly divided into 7 groups (n = 6). The **Rh-1** was administered via intraperitoneal injection at the specified doses once a day for 12 days. The animals were closely monitored for any signs of toxicity, and their body weights were recorded daily.

Subcutaneous xenograft models were established by injecting 8×10^4 4T1 cells into immunocompetent female BALB/c mice (7 mice per group). When the tumor volume grown to about 60 mm^3, cisplatin (2 mg/kg) and **Rh-1** (6 mg/kg) were injected intraperitoneally every 2 days. Tumor volumes were monitored by digital calipers every 3 days, and calculated volume with the formula: tumor volume = (shortest diameter)^2 × (longest diameter) × 0.5. The growth curves of tumor were drawn with the average tumor volume to the number of days. All mice were euthanized when the tumor volume grown to approximately 2×10^3 mm^3. The inhibition rates of tumor growth (IRT) were figured out with the formula: IRT = 100% × (mean tumor weight of the control group−mean tumor weight of the experimental group)/mean tumor weight of the control group.

The rat monoclonal antibody (mAb; BioLegend, San Diego, CA), antimouse PD-1 (RMP1-14) or the rat immunoglobulin G2a (IgG2a; RTK2758) mAb (BioLegend) was injected intraperitoneally with dose of 200 μg/mouse on days 7, 10, and 13. For the experiment of $CD8^+$ T cell blocking, the dose 100 μg/mouse of anti-CD8 (Lyt 3.2) mAb (BioXCell) was injected intraperitoneally on days −2 and 0, and

https://doi.org/10.1021/acs.jmedchem.4c00583
J. Med. Chem. 2024, 67, 13778−13787

then every 7 days. To block CCL4, 50 μg anti-CCL4 (#46907) mAb (R&D Systems) or control rat IgG2a (#54447) mAb (R&D Systems) was administered intraperitoneally 7 days after tumor inoculation and then every 3 days. Tumors were harvested on day 14 for the preparation of TILs, which were analyzed with flow cytometry. All mouse experiments were approved by the Committee for Animal Experimentation of Guangxi Normal University (approval number: 201903-012).

4.5. Flow Cytometric Analysis of Tumor-Infiltrating Lymphocytes. A tumor-infiltrating lymphocyte (TIL) enrichment protocol was used for mouse tumors. Tumors were weighed, cut, and placed in collagenase type I and incubated on a shaker at 37 °C for 30 min. The dissociated tumor was then filtered (70 mm) to get a single-cell suspension. TILs were enriched from the single-cell suspension using a sucrose gradient (40%/70% Percoll; GE Healthcare). Mouse TILs were stained with the following directly labeled antibodies (all from BioLegend): anti-CD3e (145-2c11), anti-CD4 (RM4-5), anti-CD8a (53−6.7), anti-Ki67 (16A8), anti-PDL1 (10F.9G2), anti-FoxP3 (MF-14), and antigranzyme B (GB11).

4.6. Statistics. The data processing included the Student's *t*-test, with $p \leq 0.05$ considered significant, using SPSS 13.0.

■ ASSOCIATED CONTENT

Supporting Information

The Supporting Information is available free of charge at https://pubs.acs.org/doi/10.1021/acs.jmedchem.4c00583.

Molecular formula strings and biological data (CSV)

Crystallographic data for complex Rh-1 (CIF)

Crystallographic data for complex Rh-5 (CIF)

The methods of some experiments; ^{1}H and ^{13}C NMR spectra of all complexes synthesized in this work; ESI-MS spectra of complexes; X-ray crystallographic data of complexes Rh-1 and Rh-5; stability and UV/vis absorption spectrograms of complexes **Rh-1** and **Rh-2** in aqueous solution; IC_{50} values in several cell lines; expression levels of proteins related to ER-stress, TrxR, GR, GPx and β-catenin; results of *in vivo* mouse studies and immunohistochemistry analyses; flow cytometry analysis of apoptosis-related proteins; Western blot analysis of the relationship between ROS and apoptosis (PDF)

Crystallographic data for the structural analysis have been deposited in the Cambridge Crystallographic Data Centre, CCDC No. 2166861 and 2172152 for **Rh-1** and **Rh-5**. The data can be obtained free of charge at http://www.ccdc.cam.ac.uk, or from the Cambridge Crystallographic Data Centre, 12 Union Road, Cambridge CB21EZ, UK; fax: (+44) 1223-336-033; E-mail: deposit@ccdc.cam.ac.uk.

■ AUTHOR INFORMATION

Corresponding Authors

Ke-Bin Huang − *State Key Laboratory for Chemistry and Molecular Engineering of Medicinal Resources, Key Laboratory for Chemistry and Molecular Engineering of Medicinal Resources (Ministry of Education of China), Collaborative Innovation Center for Guangxi Ethnic Medicine, School of Chemistry and Pharmaceutical Sciences, Guangxi Normal University, Guilin 541004, China;* orcid.org/0000-0003-4773-4442; Email: kbhuang@mailbox.gxnu.edu.cn

Taotao Zou − *Guangdong Key Laboratory of Chiral Molecule and Drug Discovery, School of Pharmaceutical Science, Sun Yat-Sen University, Guangzhou 510006, China;* orcid.org/0000-0001-9129-4398; Email: zoutt3@mail.sysu.edu.cn

Hong Liang − *State Key Laboratory for Chemistry and Molecular Engineering of Medicinal Resources, Key Laboratory for Chemistry and Molecular Engineering of Medicinal Resources (Ministry of Education of China), Collaborative Innovation Center for Guangxi Ethnic Medicine, School of Chemistry and Pharmaceutical Sciences, Guangxi Normal University, Guilin 541004, China;* Email: hliang@gxnu.edu.cn

Authors

Feng-Yang Wang − *State Key Laboratory for Chemistry and Molecular Engineering of Medicinal Resources, Key Laboratory for Chemistry and Molecular Engineering of Medicinal Resources (Ministry of Education of China), Collaborative Innovation Center for Guangxi Ethnic Medicine, School of Chemistry and Pharmaceutical Sciences, Guangxi Normal University, Guilin 541004, China*

Liang-Mei Yang − *State Key Laboratory for Chemistry and Molecular Engineering of Medicinal Resources, Key Laboratory for Chemistry and Molecular Engineering of Medicinal Resources (Ministry of Education of China), Collaborative Innovation Center for Guangxi Ethnic Medicine, School of Chemistry and Pharmaceutical Sciences, Guangxi Normal University, Guilin 541004, China*

Xiao-Lin Xiong − *Guangdong Key Laboratory of Chiral Molecule and Drug Discovery, School of Pharmaceutical Science, Sun Yat-Sen University, Guangzhou 510006, China*

Jing Yang − *State Key Laboratory for Chemistry and Molecular Engineering of Medicinal Resources, Key Laboratory for Chemistry and Molecular Engineering of Medicinal Resources (Ministry of Education of China), Collaborative Innovation Center for Guangxi Ethnic Medicine, School of Chemistry and Pharmaceutical Sciences, Guangxi Normal University, Guilin 541004, China*

Yan Yang − *Guangdong Key Laboratory of Chiral Molecule and Drug Discovery, School of Pharmaceutical Science, Sun Yat-Sen University, Guangzhou 510006, China*

Jiu-Qin Tang − *State Key Laboratory for Chemistry and Molecular Engineering of Medicinal Resources, Key Laboratory for Chemistry and Molecular Engineering of Medicinal Resources (Ministry of Education of China), Collaborative Innovation Center for Guangxi Ethnic Medicine, School of Chemistry and Pharmaceutical Sciences, Guangxi Normal University, Guilin 541004, China*

Lei Gao − *State Key Laboratory for Chemistry and Molecular Engineering of Medicinal Resources, Key Laboratory for Chemistry and Molecular Engineering of Medicinal Resources (Ministry of Education of China), Collaborative Innovation Center for Guangxi Ethnic Medicine, School of Chemistry and Pharmaceutical Sciences, Guangxi Normal University, Guilin 541004, China*

Yuan Lu − *State Key Laboratory for Chemistry and Molecular Engineering of Medicinal Resources, Key Laboratory for Chemistry and Molecular Engineering of Medicinal Resources (Ministry of Education of China), Collaborative Innovation Center for Guangxi Ethnic Medicine, School of Chemistry and Pharmaceutical Sciences, Guangxi Normal University, Guilin 541004, China*

Yuan Wang − *Guangdong Key Laboratory of Chiral Molecule and Drug Discovery, School of Pharmaceutical Science, Sun Yat-Sen University, Guangzhou 510006, China*

Complete contact information is available at:
https://pubs.acs.org/10.1021/acs.jmedchem.4c00583

Author Contributions

[§]F.-Y.W., L.-M.Y., and X.-L.X. contributed equally to this work.

Notes

The authors declare no competing financial interest.

■ ACKNOWLEDGMENTS

This work was supported by the National Nature Science Foundation of China (Grant No. 22177022) and the Natural Science Foundation of Guangxi Province of China (Grant: AD17129007).

■ ABBREVIATIONS

ATF, activating transcription factor; ATP, adenosine triphosphate; CCL4, cc chemokine ligand 4; CHOP, CCAAT/enhancer-binding protein homologous protein; CRT, calreticulin; DAMP, damage-associated molecular pattern; DKK1, dickkopf 1; eIF2a, eukaryotic initiation factor 2a; ER, endoplasmic reticulum; GPx, glutathione peroxidase; GR, glutathione reductase; HMGB1, high mobility group box 1; ICB, immune checkpoint blockade; ICD, immunogenic cell death; LEF1, lymphoid enhancer-binding factor 1; PD-1, programmed death receptor 1; PERK, protein kinase-like endoplasmic reticulum kinase; ROS, reactive oxygen species; TCF, Wnt-T cell factor; TIL, tumor-infiltrating lymphocyte; TNBC, triple-negative breast cancer

■ REFERENCES

(1) Englinger, B.; Pirker, C.; Heffeter, P.; Terenzi, A.; Kowol, C. R.; Keppler, B. K.; Berger, W. Metal Drugs and the Anticancer Immune Response. *Chem. Rev.* **2019**, *119*, 1519−1624.
(2) Terenzi, A.; Pirker, C.; Keppler, B. K.; Berger, W. Anticancer metal drugs and immunogenic cell death. *J. Inorg. Biochem.* **2016**, *165*, 71−79.
(3) Jin, S.; Muhammad, N.; Sun, Y.; Tan, Y.; Yuan, H.; Song, D.; Guo, Z.; Wang, X. Multispecific Platinum(IV) Complex Deters Breast Cancer via Interposing Inflammation and Immunosuppression as an Inhibitor of COX-2 and PD-L1. *Angew. Chem., Int. Ed.* **2020**, *59*, 23313−23321.
(4) Su, X.; Wang, W. J.; Cao, Q.; Zhang, H.; Liu, B.; Ling, Y.; Zhou, X.; Mao, Z. W. A Carbonic Anhydrase IX (CAIX)-Anchored Rhenium(I) Photosensitizer Evokes Pyroptosis for Enhanced Anti-Tumor Immunity. *Angew. Chem., Int. Ed.* **2022**, *61*, No. e202115800.
(5) Sen, S.; Won, M.; Levine, M. S.; Noh, Y.; Sedgwick, A. C.; Kim, J. S.; Sessler, J. L.; Arambula, J. F. Metal-based anticancer agents as immunogenic cell death inducers: the past, present, and future. *Chem. Soc. Rev.* **2022**, *51*, 1212−1233.
(6) Krysko, D. V.; Garg, A. D.; Kaczmarek, A.; Krysko, O.; Agostinis, P.; Vandenabeele, P. Immunogenic cell death and DAMPs in cancer therapy. *Nat. Rev. Cancer* **2012**, *12*, 860−875.
(7) Galluzzi, L.; Buque, A.; Kepp, O.; Zitvogel, L.; Kroemer, G. Immunogenic cell death in cancer and infectious disease. *Nat. Rev. Immunol.* **2017**, *17*, 97−111.
(8) Zhang, J.; Sun, X.; Zhao, X.; Yang, C.; Shi, M.; Zhang, B.; Hu, H.; Qiao, M.; Chen, D.; Zhao, X. Combining immune checkpoint blockade with ATP-based immunogenic cell death amplifier for cancer chemo-immunotherapy. *Acta Pharm. Sin. B* **2022**, *12*, 3694−3709.
(9) Zheng, D.; Liu, J.; Xie, L.; Wang, Y.; Ding, Y.; Peng, R.; Cui, M.; Wang, L.; Zhang, Y.; Zhang, C.; Yang, Z. Enzyme-instructed and mitochondria-targeting peptide self-assembly to efficiently induce immunogenic cell death. *Acta Pharm. Sin. B* **2022**, *12*, 2740−2750.
(10) Wong, D. Y. Q.; Ong, W. W.; Ang, W. H. Induction of immunogenic cell death by chemotherapeutic platinum complexes. *Angew. Chem., Int. Ed.* **2015**, *54*, 6483−6487.
(11) Tham, M. J. R.; Babak, M. V.; Ang, W. H. PlatinER: A Highly Potent Anticancer Platinum(II) Complex that Induces Endoplasmic Reticulum Stress Driven Immunogenic Cell Death. *Angew. Chem., Int. Ed.* **2020**, *59*, 19070−19078.
(12) Huang, K. B.; Wang, F. Y.; Feng, H. W.; Luo, H.; Long, Y.; Zou, T.; Chan, A. S. C.; Liu, R.; Zou, H.; Chen, Z. F.; Liu, Y. C.; Liu, Y. N.; Liang, H. An aminophosphonate ester ligand-containing platinum(ii) complex induces potent immunogenic cell death in vitro and elicits effective anti-tumour immune responses in vivo. *Chem. Commun.* **2019**, *55*, 13066−13069.
(13) Sen, S.; Hufnagel, S.; Maier, E. Y.; Aguilar, I.; Selvakumar, J.; DeVore, J. E.; Lynch, V. M.; Arumugam, K.; Cui, Z.; Sessler, J. L.; Arambula, J. F. Rationally Designed Redox-Active Au(I) N-Heterocyclic Carbene: An Immunogenic Cell Death Inducer. *J. Am. Chem. Soc.* **2020**, *142*, 20536−20541.
(14) Wernitznig, D.; Meier-Menches, S. M.; Cseh, K.; Theiner, S.; Wenisch, D.; Schweikert, A.; Jakupec, M. A.; Koellensperger, G.; Wernitznig, A.; Sommergruber, W.; Keppler, B. K. Plecstatin-1 induces an immunogenic cell death signature in colorectal tumour spheroids. *Metallomics* **2020**, *12*, 2121−2133.
(15) Kaur, P.; Johnson, A.; Northcote-Smith, J.; Lu, C.; Suntharalingam, K. Immunogenic Cell Death of Breast Cancer Stem Cells Induced by an Endoplasmic Reticulum-Targeting Copper(II) Complex. *Chembiochem* **2020**, *21*, 3618−3624.
(16) Bian, M.; Fan, R.; Yang, Z.; Chen, Y.; Xu, Z.; Lu, Y.; Liu, W. Pt(II)-NHC Complex Induces ROS-ERS-Related DAMP Balance to Harness Immunogenic Cell Death in Hepatocellular Carcinoma. *J. Med. Chem.* **2022**, *65*, 1848−1866.
(17) Vigueras, G.; Markova, L.; Novohradsky, V.; Marco, A.; Cutillas, N.; Kostrhunova, H.; Kasparkova, J.; Ruiz, J.; Brabec, V. A photoactivated Ir(iii) complex targets cancer stem cells and induces secretion of damage-associated molecular patterns in melanoma cells characteristic of immunogenic cell death. *Inorg. Chem. Front.* **2021**, *8*, 4696−4711.
(18) Yamazaki, T.; Buque, A.; Ames, T. D.; Galluzzi, L. PT-112 induces immunogenic cell death and synergizes with immune checkpoint blockers in mouse tumor models. *Oncoimmunology* **2020**, *9*, No. 1721810.
(19) Konda, P.; Lifshits, L. M.; Roque, J. A.; Cole, H. D.; Cameron, C. G.; McFarland, S. A.; Gujar, S. Discovery of immunogenic cell death-inducing ruthenium-based photosensitizers for anticancer photodynamic therapy. *OncoImmunology* **2021**, *10*, No. 1863626.
(20) Sabbatini, M.; Zanellato, I.; Ravera, M.; Gabano, E.; Perin, E.; Rangone, B.; Osella, D. Pt(IV) Bifunctional Prodrug Containing 2-(2-Propynyl)octanoato Axial Ligand: Induction of Immunogenic Cell Death on Colon Cancer. *J. Med. Chem.* **2019**, *62*, 3395−3406.
(21) Novohradsky, V.; Pracharova, J.; Kasparkova, J.; Imberti, C.; Bridgewater, H. E.; Sadler, P. J.; Brabec, V. Induction of immunogenic cell death in cancer cells by a photoactivated platinum(iv) prodrug. *Inorg. Chem. Front.* **2020**, *7*, 4150−4159.
(22) Wernitznig, D.; Kiakos, K.; Del Favero, G.; Harrer, N.; Machat, H.; Osswald, A.; Jakupec, M. A.; Wernitznig, A.; Sommergruber, W.; Keppler, B. K. First-in-class ruthenium anticancer drug (KP1339/IT-139) induces an immunogenic cell death signature in colorectal spheroids in vitro†. *Metallomics* **2019**, *11*, 1044−1048.
(23) Sun, Y.; Yin, E.; Tan, Y.; Yang, T.; Song, D.; Jin, S.; Guo, Z.; Wang, X. Immunogenicity and cytotoxicity of a platinum(iv) complex derived from capsaicin. *Dalton Trans.* **2021**, *50*, 3516−3522.
(24) Huang, K.-B.; Wang, F.-Y.; Lu, Y.; Yang, L.-M.; Long, N.; Wang, S.-S.; Xie, Z.; Levine, M.; Zou, T.; Sessler, J. L.; Liang, H. Cu(II) complex that synergistically potentiates cytotoxicity and an antitumor immune response by targeting cellular redox homeostasis. *Proc. Natl. Acad. Sci. U.S.A.* **2024**, *121*, No. e2404668121.
(25) Lu, Y.; Wang, S.-S.; Li, M.-Y.; Liu, R.; Zhu, M.-F.; Yang, L.-M.; Wang, F.-Y.; Huang, K.-B.; Liang, H. Cyclometalated iridium(III) complex based on isoquinoline alkaloid synergistically elicits the ICD

response and IDO inhibition via autophagy-dependent ferroptosis *Acta Pharm. Sin. B* 2024, DOI: 10.1016/j.apsb.2024.06.017.
(26) Wang, L.; Guan, R.; Xie, L.; Liao, X.; Xiong, K.; Rees, T. W.; Chen, Y.; Ji, L.; Chao, H. An ER-Targeting Iridium(III) Complex That Induces Immunogenic Cell Death in Non-Small-Cell Lung Cancer. *Angew. Chem., Int. Ed.* **2021**, *60*, 4657−4665.
(27) Kepp, O.; Zitvogel, L.; Kroemer, G. Clinical evidence that immunogenic cell death sensitizes to PD-1/PD-L1 blockade. *OncoImmunology* **2019**, *8*, No. e1637188.
(28) Kepp, O.; Kroemer, G. A novel platinum-based chemotherapeutic inducing immunogenic cell death. *Oncoimmunology* **2020**, *9*, No. 1729022.
(29) Su, X.; Liu, B.; Wang, W. J.; Peng, K.; Liang, B. B.; Zheng, Y.; Cao, Q.; Mao, Z. W. Disruption of Zinc Homeostasis by a Novel Platinum(IV)-Terthiophene Complex for Antitumor Immunity. *Angew. Chem., Int. Ed.* **2023**, *62*, No. e202216917.
(30) Yang, J.; Yang, B.; Shi, J. A Nanomedicine-Enabled Ion-Exchange Strategy for Enhancing Curcumin-Based Rheumatoid Arthritis Therapy. *Angew. Chem., Int. Ed.* **2023**, *62*, No. e202310061.
(31) Ji, Z. S.; Gao, G. B.; Ma, Y. M.; Luo, J. X.; Zhang, G. W.; Yang, H.; Li, N.; He, Q. Y.; Lin, H. S. Highly bioactive iridium metal-complex alleviates spinal cord injury via ROS scavenging and inflammation reduction. *Biomaterials* **2022**, *284*, No. 121481.
(32) Kang, T. S.; Ko, C. N.; Zhang, J. T.; Wu, C.; Wong, C. Y.; Ma, D. L.; Leung, C. H. Rhodium(III)-Based Inhibitor of the JMJD3-H3K27me3 Interaction and Modulator of the Inflammatory Response. *Inorg. Chem.* **2018**, *57*, 14023−14026.
(33) Zhong, H. J.; Wang, W.; Kang, T. S.; Yan, H.; Yang, Y.; Xu, L.; Wang, Y.; Ma, D. L.; Leung, C. H. A Rhodium(III) Complex as an Inhibitor of Neural Precursor Cell Expressed, Developmentally Down-Regulated 8-Activating Enzyme with in Vivo Activity against Inflammatory Bowel Disease. *J. Med. Chem.* **2017**, *60*, 497−503.
(34) Gerard, C. L.; Delyon, J.; Wicky, A.; Homicsko, K.; Cuendet, M. A.; Michielin, O. Turning tumors from cold to inflamed to improve immunotherapy response. *Cancer Treat Rev.* **2021**, *101*, No. 102227.
(35) Trujillo, J. A.; Sweis, R. F.; Bao, R.; Luke, J. J. T Cell-Inflamed versus Non-T Cell-Inflamed Tumors: A Conceptual Framework for Cancer Immunotherapy Drug Development and Combination Therapy Selection. *Cancer Immunol. Res.* **2018**, *6*, 990−1000.
(36) Anandappa, A. J.; Wu, C. J.; Ott, P. A. Directing Traffic: How to Effectively Drive T Cells into Tumors. *Cancer Discovery* **2020**, *10*, 185−197.
(37) Waldman, A. D.; Fritz, J. M.; Lenardo, M. J. A guide to cancer immunotherapy: from T cell basic science to clinical practice. *Nat. Rev. Immunol.* **2020**, *20*, 651−668.
(38) Sharma, P.; Hu-Lieskovan, S.; Wargo, J. A.; Ribas, A. Primary, Adaptive, and Acquired Resistance to Cancer Immunotherapy. *Cell* **2017**, *168*, 707−723.
(39) Patel, S. A.; Minn, A. J. Combination Cancer Therapy with Immune Checkpoint Blockade: Mechanisms and Strategies. *Immunity* **2018**, *48*, 417−433.
(40) Spranger, S.; Bao, R.; Gajewski, T. F. Melanoma-intrinsic beta-catenin signalling prevents anti-tumour immunity. *Nature* **2015**, *523*, 231−235.
(41) Luke, J. J.; Bao, R.; Sweis, R. F.; Spranger, S.; Gajewski, T. F. WNT/beta-catenin Pathway Activation Correlates with Immune Exclusion across Human Cancers. *Clin. Cancer Res.* **2019**, *25*, 3074−3083.
(42) Ruiz de Galarreta, M.; Bresnahan, E.; Molina-Sanchez, P.; Lindblad, K. E.; Maier, B.; Sia, D.; Puigvehi, M.; Miguela, V.; Casanova-Acebes, M.; Dhainaut, M.; Villacorta-Martin, C.; Singhi, A. D.; Moghe, A.; von Felden, J.; Tal Grinspan, L.; Wang, S.; Kamphorst, A. O.; Monga, S. P.; Brown, B. D.; Villanueva, A.; Llovet, J. M.; Merad, M.; Lujambio, A. beta-Catenin Activation Promotes Immune Escape and Resistance to Anti-PD-1 Therapy in Hepatocellular Carcinoma. *Cancer Discovery* **2019**, *9*, 1124−1141.
(43) Berraondo, P.; Ochoa, M. C.; Olivera, I.; Melero, I. Immune Desertic Landscapes in Hepatocellular Carcinoma Shaped by beta-Catenin Activation. *Cancer Discovery* **2019**, *9*, 1003−1005.
(44) Li, X.; Xiang, Y.; Li, F.; Yin, C.; Li, B.; Ke, X. WNT/beta-Catenin Signaling Pathway Regulating T Cell-Inflammation in the Tumor Microenvironment. *Front. Immunol.* **2019**, *10*, No. 2293.
(45) Sun, Q.; Wang, Y.; Fu, Q.; Ouyang, A.; Liu, S.; Wang, Z.; Su, Z.; Song, J.; Zhang, Q.; Zhang, P.; Lu, D. Sulfur-Coordinated Organoiridium(III) Complexes Exert Breast Anticancer Activity via Inhibition of Wnt/beta-Catenin Signaling. *Angew. Chem., Int. Ed.* **2021**, *60*, 4841−4848.
(46) Chow, K. H.; Sun, R. W.; Lam, J. B.; Li, C. K.; Xu, A.; Ma, D. L.; Abagyan, R.; Wang, Y.; Che, C. M. A gold(III) porphyrin complex with antitumor properties targets the Wnt/beta-catenin pathway. *Cancer Res.* **2010**, *70*, 329−337.
(47) Sohrabi, M.; Saeedi, M.; Larijani, B.; Mahdavi, M. Recent advances in biological activities of rhodium complexes: Their applications in drug discovery research. *Eur. J. Med. Chem.* **2021**, *216*, No. 113308.
(48) Hanif, M.; Arshad, J.; Astin, J. W.; Rana, Z.; Zafar, A.; Movassaghi, S.; Leung, E.; Patel, K.; Sohnel, T.; Reynisson, J.; Sarojini, V.; Rosengren, R. J.; Jamieson, S. M. F.; Hartinger, C. G. A Multitargeted Approach: Organorhodium Anticancer Agent Based on Vorinostat as a Potent Histone Deacetylase Inhibitor. *Angew. Chem., Int. Ed.* **2020**, *59*, 14609−14614.
(49) Boyle, K. M.; Barton, J. K. A Family of Rhodium Complexes with Selective Toxicity toward Mismatch Repair-Deficient Cancers. *J. Am. Chem. Soc.* **2018**, *140*, 5612−5624.
(50) Boyle, K. M.; Nano, A.; Day, C.; Barton, J. K. Cellular Target of a Rhodium Metalloinsertor is the DNA Base Pair Mismatch. *Chem. - Eur. J.* **2019**, *25*, 3014−3019.
(51) Komor, A. C.; Barton, J. K. An unusual ligand coordination gives rise to a new family of rhodium metalloinsertors with improved selectivity and potency. *J. Am. Chem. Soc.* **2014**, *136*, 14160−14172.
(52) Maheswari, P. U.; Barends, S.; Ozalp-Yaman, S.; de Hoog, P.; Casellas, H.; Teat, S. J.; Massera, C.; Lutz, M.; Spek, A. L.; van Wezel, G. P.; Gamez, P.; Reedijk, J. Unique ligand-based oxidative DNA cleavage by zinc(II) complexes of hpyramol and hpyrimol. *Chem. - Eur. J.* **2007**, *13*, 5213−5222.
(53) Pachón, L. D.; Golobič, A.; Kozlevčar, B.; Gamez, P.; Kooijman, H.; Spek, A. L.; Reedijk, J. Intramolecular oxidation of the ligand 4-methyl-2-N-(2-pyridylmethyl)aminophenol (Hpyramol) upon coordination with iron(II) chloride and manganese(II) perchlorate. *Inorg. Chim. Acta* **2004**, *357*, 3697−3702.
(54) Maheswari, P. U.; Roy, S.; den Dulk, H.; Barends, S.; van Wezel, G.; Kozlevcar, B.; Gamez, P.; Reedijk, J. The square-planar cytotoxic [Cu(II)(pyrimol)Cl] complex acts as an efficient DNA cleaver without reductant. *J. Am. Chem. Soc.* **2006**, *128*, 710−711.
(55) King, A. P.; Wilson, J. J. Endoplasmic reticulum stress: an arising target for metal-based anticancer agents. *Chem. Soc. Rev.* **2020**, *49*, 8113−8136.
(56) Huang, C.; Li, T.; Liang, J.; Huang, H.; Zhang, P.; Banerjee, S. Recent advances in endoplasmic reticulum targeting metal complexes. *Coord. Chem. Rev.* **2020**, *408*, No. 213178.
(57) Huang, W.; Pan, C.; Huang, Y.; Huang, T.; Dong, X.; Chen, Y.; Shi, H.; Lau, T.; Man, W.; Ni, W. (Salen)osmium(VI) nitrides catalyzed glutathione depletion in chemotherapy. *Chin. Chem. Lett.* **2023**, *34*, No. 108153.
(58) Ramos, R.; Gilles, J. F.; Morichon, R.; Przybylski, C.; Caron, B.; Botuha, C.; Karaiskou, A.; Salmain, M.; Sobczak-Thepot, J. Cytotoxic BODIPY-Appended Half-Sandwich Iridium(III) Complex Forms Protein Adducts and Induces ER Stress. *J. Med. Chem.* **2021**, *64*, 16675−16686.
(59) Wek, R. C.; Jiang, H. Y.; Anthony, T. G. Coping with stress: eIF2 kinases and translational control. *Biochem. Soc. Trans.* **2006**, *34*, 7−11.
(60) Han, J.; Back, S. H.; Hur, J.; Lin, Y. H.; Gildersleeve, R.; Shan, J.; Yuan, C. L.; Krokowski, D.; Wang, S.; Hatzoglou, M.; Kilberg, M. S.; Sartor, M. A.; Kaufman, R. J. ER-stress-induced transcriptional

regulation increases protein synthesis leading to cell death. *Nat. Cell Biol.* **2013**, *15*, 481−490.
(61) Horndasch, M.; Lienkamp, S.; Springer, E.; Schmitt, A.; Pavenstadt, H.; Walz, G.; Gloy, J. The C/EBP homologous protein CHOP (GADD153) is an inhibitor of Wnt/TCF signals. *Oncogene* **2006**, *25*, 3397−3407.
(62) Costa, R.; Peruzzo, R.; Bachmann, M.; Monta, G. D.; Vicario, M.; Santinon, G.; Mattarei, A.; Moro, E.; Quintana-Cabrera, R.; Scorrano, L.; Zeviani, M.; Vallese, F.; Zoratti, M.; Paradisi, C.; Argenton, F.; Brini, M.; Cali, T.; Dupont, S.; Szabo, I.; Leanza, L. Impaired Mitochondrial ATP Production Downregulates Wnt Signaling via ER Stress Induction. *Cell Rep.* **2019**, *28*, 1949−1960 e6.
(63) Jeon, S. M.; Chandel, N. S.; Hay, N. AMPK regulates NADPH homeostasis to promote tumour cell survival during energy stress. *Nature* **2012**, *485*, 661−665.
(64) Someya, S.; Yu, W.; Hallows, W. C.; Xu, J.; Vann, J. M.; Leeuwenburgh, C.; Tanokura, M.; Denu, J. M.; Prolla, T. A. Sirt3 mediates reduction of oxidative damage and prevention of age-related hearing loss under caloric restriction. *Cell* **2010**, *143*, 802−812.
(65) Rahman, I.; Kode, A.; Biswas, S. K. Assay for quantitative determination of glutathione and glutathione disulfide levels using enzymatic recycling method. *Nat. Protoc.* **2006**, *1*, 3159−3165.
(66) Holmström, K. M.; Finkel, T. Cellular mechanisms and physiological consequences of redox-dependent signalling. *Nat. Rev. Mol. Cell Biol.* **2014**, *15*, 411−421.
(67) Gorrini, C.; Harris, I. S.; Mak, T. W. Modulation of oxidative stress as an anticancer strategy. *Nat. Rev. Drug Discovery* **2013**, *12*, 931−947.
(68) Sies, H.; Jones, D. P. Reactive oxygen species (ROS) as pleiotropic physiological signalling agents. *Nat. Rev. Mol. Cell Biol.* **2020**, *21*, 363−383.
(69) Lu, Y.; Liu, Y.; Liang, Z.; Ma, X.; Liu, L.; Wen, Z.; Tolbatov, I.; Marrone, A.; Liu, W. NHC-gold(I)-alkyne complexes induced hepatocellular carcinoma cell death through bioorthogonal activation by palladium complex in living system. *Chin. Chem. Lett.* **2023**, *34*, No. 108413.
(70) Feng, B.; Zhang, Y.; Liu, T.; Chan, L.; Chen, T.; Zhao, J. Selenium speciation determines the angiogenesis effect through regulating selenoproteins to trigger ROS-mediated cell apoptosis and cell cycle arrest. *Chin. Chem. Lett.* **2023**, *34*, No. 108264.
(71) Zou, T.; Lum, C. T.; Lok, C. N.; Zhang, J. J.; Che, C. M. Chemical biology of anticancer gold(III) and gold(I) complexes. *Chem. Soc. Rev.* **2015**, *44*, 8786−8801.
(72) Yang, W.; Xiu, Z.; He, Y.; Huang, W.; Li, Y.; Sun, T. Bip inhibition in glioma stem cells promotes radiation-induced immunogenic cell death. *Cell Death Dis.* **2020**, *11*, No. 786.
(73) Huang, K. C.; Chiang, S. F.; Yang, P. C.; Ke, T. W.; Chen, T. W.; Lin, C. Y.; Chang, H. Y.; Chen, W. T.; Chao, K. C. ATAD3A stabilizes GRP78 to suppress ER stress for acquired chemoresistance in colorectal cancer. *J. Cell. Physiol.* **2021**, *236*, 6481−6495.

https://doi.org/10.1021/acs.jmedchem.4c00583
J. Med. Chem. 2024, 67, 13778−13787